CHAPTER II
REVIEW OF THE LITERATURE

The review is divided into four major parts as follows:

2.1 Amelogenesis

2.1.1 Presecretory stage

2.1.2 Secretory stage

2.1.3 Maturation stage

2.2 Enamel proteins

2.2.1 Amelogenins

2.2.2 Nonamelogenins

2.2.2.1 Enamelin

2.2.2.2 Ameloblastin

2.2.2.3 Tuftelin

2.3 Amelogenesis imperfecta

2.3.1 Definition

2.3.2 Epidemiology

2.3.3 Clinical feature

2.3.4 Classification

2.4 Etiology and candidate genes

2.4.1 Amelogenin gene (*AMEL*)

2.4.2 Matrix metalloproteinase gene (*MMP-20*)

2.4.3 Kallikrein-4 gene (*KLK4*)

2.4.4 Family with sequence similarity, member H gene (*FAM83H*)

2.4.5 Enamelin gene (*ENAM*)

2.4.5.1 *ENAM* and its structure

2.4.5.2 Mutations in *ENAM*

Amelogenesis imperfecta (AI) is a hereditary defect of enamel formation, which is not associated with other tissues (Wright, 2006). The enamel defects, which affect both primary and permanent dentitions (Aldred and Crawford, 1995), are expressed in a variety of phenotypes. Deficiency in enamel thickness (hypoplastic AI) or mineralization defects in enamel (hypocalcified AI and hypomaturation AI) are both clinical manifestations of AI (Wright et al., 2003). AI can be transmitted by either X-linked, autosomal dominant, autosomal recessive, or sporadic patterns (Backman, 1997; Aldred et al., 2003). Currently, there are many proved candidate genes related to the etiology of AI, such as amelogenin (*AMELX*), enamelin (*ENAM*), kallikrein (*KLK4*), enamelysin (*MMP20*) and the family with sequence similarity 83 member H (*FAM83H*) gene.

2.1 Amelogenesis

Amelogenesis, a complex process of creating fully mineralized enamel in the crowns, takes place at the same time as dentine formation (Smith and Nanci, 1995; Simmer and Hu, 2001). Both of the formation processes occur along the line which will finally become the dentino-enamel junction (DEJ) (Simmer and Hu, 2001). Dental enamel is a complex structure, composed 96% of mineral and 4% of organic material and water. The inorganic material is calcium phosphate (hydroxyapatite) substituted with carbonate ions (Nanci, 2008). This highly mineralized tissue is formed by the ameloblasts through three different stages: presecretory, secretory and maturation stages (Smith and Nanci, 1995; Nanci, 2008) (Figure 2.1).

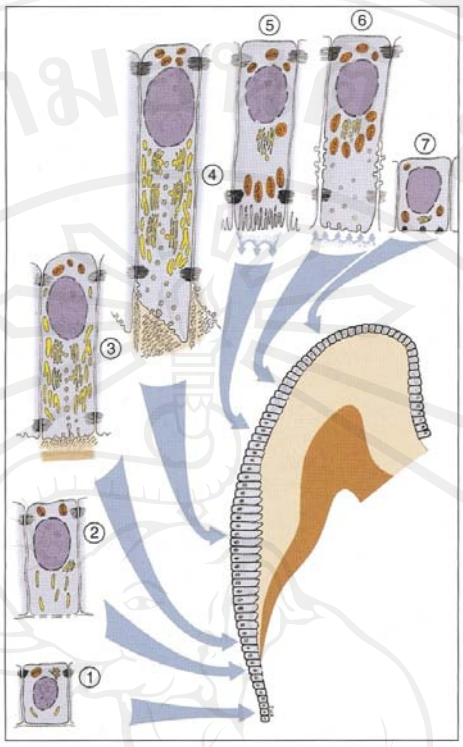

Figure 2.1 Cycle of ameloblasts in amelogenesis. (1-2) presecretory stage, (3-4) secretory stage, (5-7) maturation stage (Nanci, 2008).

2.1.1 Presecretory stage

After cuspal formation in the bell stage of tooth development, the cells of the inner enamel epithelium differentiate into ameloblasts (Nanci, 2008). The differentiation of the odontoblasts and underlying predentin induce the volume and structural changes in ameloblasts. The ameloblasts increase in both cell height and cytoplasmic volume. The Golgi apparatus and rough endoplasmic reticulum in the cytoplasm also increase in volume (Smith and Nanci, 1995). As the ameloblasts differentiate, small amounts of the enamel proteins are secreted from their apical surfaces (Inai et al., 1991; Nakamura et al., 1994).

2.1.2 Secretory stage

In secretory stage ameloblasts, the cytoplasm is highly polarized and the ameloblasts increase the amount of the Golgi apparatus and rough endoplasmic reticulum. The proximal cytoplasm contains many mitochondria, whereas the distal cytoplasm is filled with Golgi's apparatus and rough endoplasmic reticulum (Nanci,

2008). There is a rapid secretion of large amounts of enamel proteins from the apical surfaces of the cells which accumulate on top of the mineralzed mental dentin as an initial rodless (aprismatic) layer (Warshawsky, 1978; Smith et al., 1992). After the initial layer forms, the ameloblasts develop a protruding cytoplasmic process at the apical end, called Tomes' process, whereas the protein matrix is synthesized in the rough endoplasmic reticulum, and migrates to the Golgi apparatus (Warshawsky, 1978; Nanci, 2008). The protein matrix is condensed and packed in the form of membrane-bound granules and secreted through Tomes' process (Nanci, 2008) (Figure 2.2).

2.1.3 Maturation stage

The maturation stage takes two thirds of the enamel formation time. In this stage, after the final enamel layer reaches its full thickness, the ameloblasts change in both cell size and morphological characteristics because the protein and water from the matrix are removed and replaced with inorganic materials (Smith and Nanci, 1995). The morphology of the ameloblasts changes to a shorter height with a slightly broader width, whereas the excess cytoplasmic contents including Golgi's apparatus and rough endoplasmic reticulum are shed (Smith and Nanci, 1995). In this stage, 25% of the ameloblasts die during postsecretory transition, while another 25% disappear as the enamel matures (Smith and Warshawsky, 1977). Maturation stage ameloblasts undergo modulation, in which their apical surface cycles between being ruffle-ended and smooth-ended and secrete proteolytic enzymes, such as serine proteinase and enamelysin to remove protein matrix (Smith et al., 1987; Smith and Nanci, 1995). The ruffle-ended apical surface type is formed by invagination of the cell membrane to remove the enamel matrix by endocytosis using energy from the mitochondria, whereas the smooth-ended type shows little endocytotic activity (Nanci, 2008). After the protein matrix is removed, hydroxyapatite replaces the protein (Figure 2). When the enamel is fully mature, the ameloblasts stop their modulation and undergo regression as do other cells of the enamel organ. The intracellular cytoplasm and organelles decrease in volume. The cells of the reduced enamel organ help isolate the mature enamel from the surrounding connective tissue (Smith and Nanci, 1995).

2.2 Enamel proteins

Enamel proteins play important roles in enamel crystal formation. Without enamel extracellular matrix, the enamel crystal cannot grow in vitro (Hu et al., 2005). Ninety per cent of the enamel proteins are amelogenin, whereas the remaining 10% are nonamelogenin (Nanci, 2008).

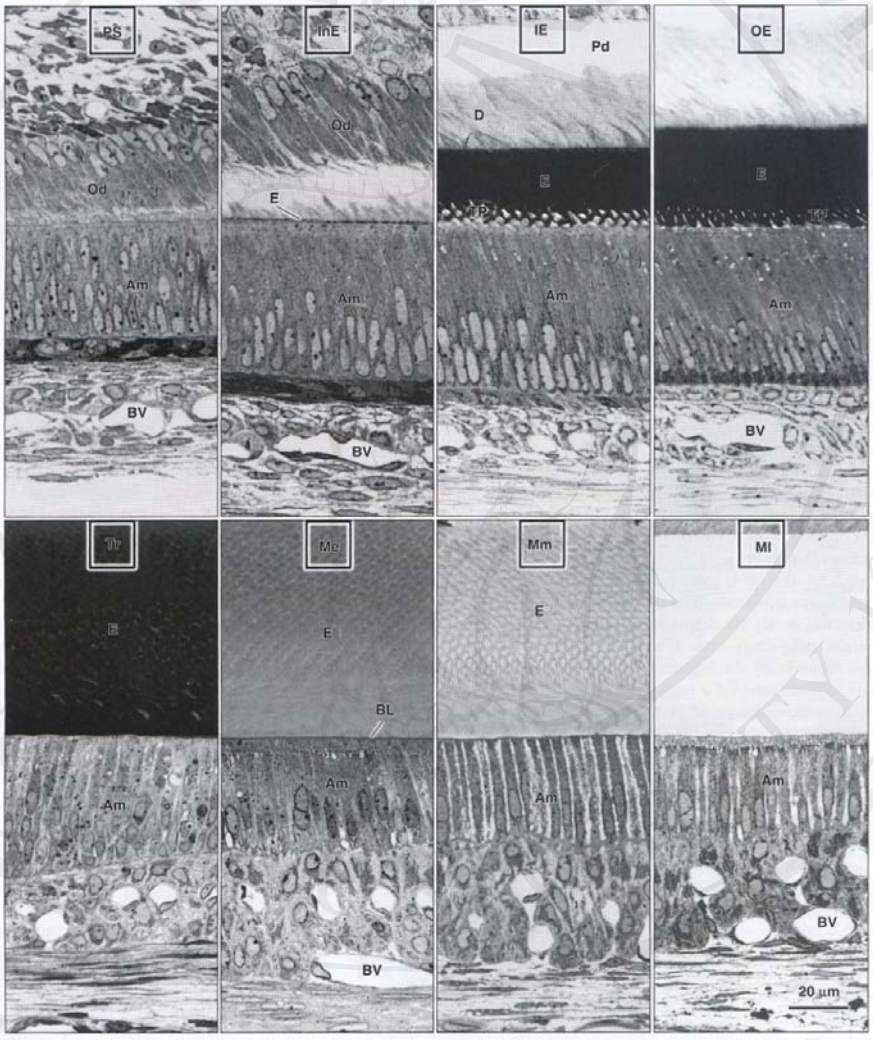

Figure 2.2 Changes in morphology of rat ameloblasts during amelogenesis. (Am) Ameloblasts, (BL) basal lamina, (D) dentin, (E) enamel, (IE) secretory stage inner enamel, (InE) secretory stage initial enamel, (Me) early maturation stage, (MI) late maturation stage, (Mm) midmaturation stage, (Od) odontoblasts, (OE) secretory stage outer enamel, (PS) presecretory stage, (TP) Tomes' process (Tr) maturation stage transition (Nanci, 2008).

2.2.1 Amelogenins

Most of the composition of the enamel proteins is amelogenin, which is a unique, tissue-specific protein in developing enamel. This protein is synthesized from the cells differentiated from the enamel organ epithelia (Slavkin et al., 1988; Snead et al., 1988). The molecular weight of amelogenin has been reported as ranging from 5 to 45 kDa (Nanci, 2008). These hydrophobic proteins are composed of high amounts of proline (25-30%), histidine, glutamine and leucine (Stephanopoulos et al., 2005; Nanci, 2008). There is a hydrophilic motif at the 12-carboxy-terminal of the proteins, which makes the protein bipolar (Snead et al., 1985). Experiments in mice have shown the expression of amelogenin in secretory, transition and early maturation stages of enamel formation (Hu et al., 2001a). Amelogenin plays a crucial role in crystal seeding and elongation in appositional growth of the enamel (Fincham et al., 1994; Fincham et al., 1995).

2.2.2 Nonamelogenins

Nonamelogenin proteins, such as enamelin, ameloblastin and tuftelin, comprise 10% of the enamel protein composition. It is believed that nonamelogenin proteins help in promoting and guiding the formation of the enamel crystal (Nanci, 2008).

2.2.2.1 Enamelin

From one to five per cent of the enamel protein amount is enamelin, which is the largest known enamel protein, with 1,104 amino acids and a 39-amino-acid signaling peptide (Fukae et al., 1996; Hu et al., 2000a; Hu et al., 2001b; Hu et al., 2005). Enamelin expression has been found in the three stages of enamel formation in mouse experimental studies (Hu et al., 2001a). Before the expression of amelogenin, the enamelin expression is terminated (Hu et al., 2001a). Most of the protein degrades and it is reabsorbed rapidly after its secretion (Hu and Yamakoshi, 2003). Enamelin functions in crystal nucleation and growth (Nanci, 2008).

2.2.2.2 Ameloblastin

Ameloblastin, also known as amelin (Cerny et al., 1996) and sheathlin (Hu et al., 1997), is composed of high amounts of proline, leucine and glycine (Stephanopoulos et al., 2005). This hydrophilic protein roughly accounts for 5% of enamel proteins

(Stephanopoulos et al., 2005). Ameloblastin is a bipolar molecule with a basic N-terminal side and an acidic C-terminal side (Hu et al., 2005). It has been reported that without ameloblastin in knockout mice, there is no enamel layer formation (Fukumoto et al., 2004). It is suggested that this protein helps in promoting mineral formation and crystal elongation (Nanci, 2008).

2.2.2.3 Tuftelin

Tuftelin is another enamel protein which is present in small amounts. It is highly expressed in the dentino-enamel junction area, which is an unusual area for the expression of amelogenin and other nonamelogenin proteins (Deutsch et al., 1991; Deutsch et al., 1995a; Deutsch et al., 1995b; Zeichner-David et al., 1995). It is suggested that tuftelin helps in inductive events for mineralization of the enamel near the dentino-enamel junction but it is unlikely to help in controlling crystal growth as the enamel matures (Zeichner-David et al., 1997).

2.3 Amelogenesis imperfecta

2.3.1 Definition

AI is a hereditary defect of dental enamel which affects both primary and permanent dentitions resulting in generalized abnormal enamel formation without other organ disorders (Witkop, 1988; Aldred and Crawford, 1995).

2.3.2 Epidemiology

Variations in the distribution of AI in different populations depend on the gene pool (Crawford et al., 2007). The incidence has been reported as ranging from 1: 14,000 in the US (Witkop, 1957) to 1:8,000 in Israel (Chosack et al., 1979) and 1: 700 in Sweden (Backman and Holm, 1986). The estimated extrapolation of the prevalence rate of amelogenesis imperfecta in Asian countries such as Japan, Hong Kong, North and South Korea, Taiwan, Pakistan, Sri Lanka, Indonesia, Laos, Malaysia, Singapore, Thailand, Vietnam is 1:14,000 (http://www.wrongdiagnosis.com /a/amelogenesis_imperfecta/stats-country.htm#extrawarning)

2.3.3 Clinical features

The clinical manifestations of the enamel defects in AI can be classified into three main types: hypoplastic, hypocalcified and hypomaturation types. The hypoplastic type shows hard enamel with normal translucency but the enamel is thin or deficient in amount, and may result in spacing between teeth. It can also result in irregular pits and grooves in fine enamel (Gopinath et al., 2004; Wright, 2006; Hu et al., 2007). The hypocalcified type presents with enamel of normal thickness, but which is soft in consistency due to low mineralization, and is pigmented (Gopinath et al., 2004). As the enamel is easily detachable after tooth eruption, the residual, thin enamel is similar to that in the hypoplastic type. The hypomaturation type shows normal thickness of enamel with mottled white opaque coloration, but the enamel is porous (Backman and Anneroth, 1989; Seow, 1993). The enamel can be orange-brown in color with reduction of radiodensity when compared with the underlying dentin (Wright, 2006).

2.3.4 Classification

As AI has phenotypic variability in clinical manifestations, many classifications have evolved. One of the classifications, which is commonly accepted, is that proposed by Witkop (Witkop, 1988) (Figure 2.3).

Witkop, 1988 [11]	*Four major categories based primarily on phenotype (hypoplastic, hypomaturation, hypocalcified, hypomaturation-hypoplastic with taurodontism) subdivided into 15 subtypes by phenotype and and secondarily by mode of inheritance.*
	Type I. Hypoplastic
	Type IA. Hypoplastic, pitted autosomal dominant
	Type IB. Hypoplastic, local autosomal dominant
	Type IC. Hypoplastic, local autosomal recessive
	Type ID. Hypoplastic, smooth autosomal dominant
	Type IE. Hypoplastic, smooth X-linked dominant
	Type IF. Hypoplastic, rough autosomal dominant
	Type IG. Enamel agenesis, autosomal recessive
	Type II. Hypomaturation
	Type IIA. Hypomaturation, pigmented autosomal recessive
	Type IIB. Hypomaturation, X-linked recessive
	Type IIC. Hypomaturation, snow-capped teeth, X-linked
	Type IID. Hypomaturation, snow-capped teeth, autosomal dominant?
	Type IIIA. Autosomal dominant
	Type IIIB. Autosomal recessive
	Type IV. Hypomaturation-hypoplastic with taurodontism
	Type IVA. Hypomaturation-hypoplastic with taurodontism, autosomal dominant
	Type IVB. Hypoplastic-hypomaturation with taurodontism, autosomal dominant

Figure 2.3 AI classification by Witkop (1988). This classification uses phenotype as the primary mode of classification and inheritance pattern as the secondary factor for diagnosis (Witkop, 1988). (For review please read Crawford et al., 2007.)

2.4 Etiology and candidate genes

Many genes play a role in enamel formation in the developing tooth, and mutations in several genes have been proved to be associated with the causes of AI.

2.4.1 Amelogenin gene (*AMEL*)

AMEL is located on Xq22 (Stephanopoulos et al., 2005). This gene codes amelogenin protein, which is the largest of the enamel proteins. *AMEL* is expressed in many cells during enamel formation, cells such as preameloblasts and ameloblasts, and in remnants of the epithelial root sheath (Fong and Hammarstrom, 2000; Hu et al., 2001a). Low expression in odontoblasts is also shown (Nagano et al., 2003; Papagerakis et al., 2003). Amelogenin is thought to form a scaffold for the developing enamel and to help in controlling the direction of crystallite growth (Robinson et al., 1990; Fincham and Simmer, 1997).

Reported phenotypic variability in *AMEL* consists of hypoplastic and hypomaturation types (Wright et al., 2003). The mutant allele is expressed in males, whereas the mosaic pattern (Lyonization) shows in females with discoloration or vertical bands in enamel due to X chromosome inactivation (Witkop, 1967). Mutations in 16-amino-acid signaling peptides of amelogenin result in thin and

smooth hypoplastic enamel (Lagerstrom-Fermer and Landegren, 1995; Sukigushi H, 2001; Kim et al., 2004) (Figure 2.4). Mutations in the N-terminus of the amelogenin protein primarily show phenotypes of hypomaturation, with various degrees of enamel hypoplasia (Lench et al., 1994; Lench and Winter, 1995; Ravassipour et al., 2000; Hart et al., 2002) (Figure 2.5). Reported mutations in the C-terminal region, which lead to a premature stop codon, result in the hypoplastic type of AI (Lench and Winter, 1995; Kindelan et al., 2000; Greene et al., 2002; Hart et al., 2002) (Figure 2.6).

Figure 2.4 Mutation in signaling peptides of amelogenin shows extremely thin enamel in both clinical manifestation and radiographs (Kim et al., 2004; Wright, 2006).

Figure 2.5 *AMEL* mutation in the N-terminus of amelogenin protein cause opaque white discoloration at the cervical area of the crowns with yellow-brown discoloration on the remainder of the crowns (Ravassipour et al., 2000).

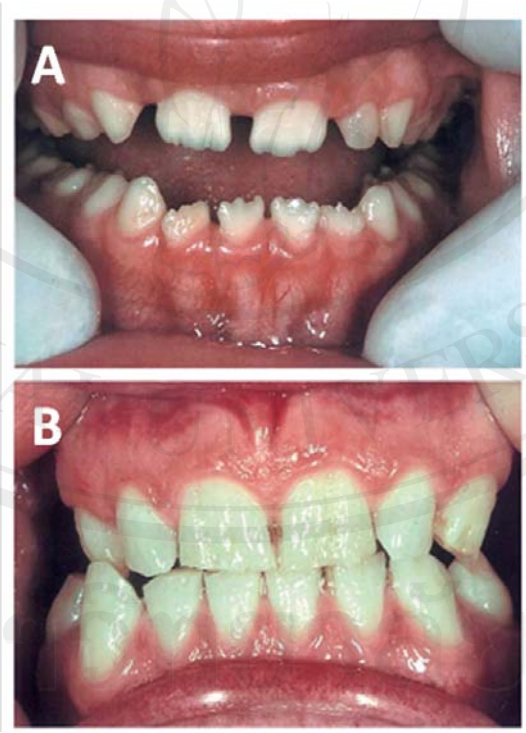

Figure 2.6 *AMEL* mutation in the C-terminus of amelogenin. (A) Affected male, with thin enamel and uniform contour in both primary and permanent dentitions. (B) Vertical grooves on enamel of heterozygous female, especially in maxillary central incisors and mandibular teeth (Hart et al., 2002).

2.4.2 Matrix metalloproteinase gene (*MMP-20*)

MMP-20 is a tooth-specific gene located in chromosome 11q22.3-q23 (Llano et al., 1997). *MMP-20* plays a role in coding for enamelysin, a calcium-dependent proteinase (Bartlett et al., 1998), which is an early protease for removing enamel protein matrix. This proteinase is a member of the matrix metalloprotidase family (MMPs) (Rawlings et al., 2004) and it is expressed in ameoblasts during the secretory and maturation stages of amelogenesis (Bartlett et al., 1996; Begue-Kirn et al., 1998; Bartlett and Simmer, 1999).

Mutations in *MMP-20* show the autosomal recessive hypomaturation type of AI as the mineral content in enamel is reduced (Kim et al., 2005b). The dental manifestations of probands with *MMP-20* mutations are: normal thickness of enamel with orange-brown coloration, enamel with little contrast on radiographs due to lack of radiopacity when compared with dentin (Kim et al., 2005b) (Figure 2.7).

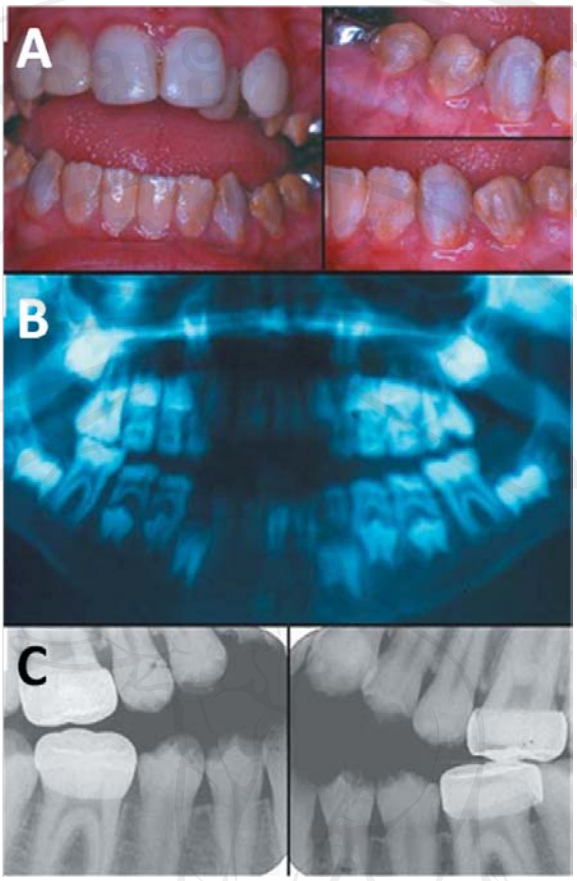

Figure 2.7 Mutations in *MMP-20* show hypomaturation enamel. (A) Frontal and lateral views of a proband present composite veneers on maxillary teeth, brown teeth with rough, mottled enamel and staining on mandibular teeth. (B) Anterior open bite is also evidenced in this proband. (C) Reduction in radiodensity of hypomaturation enamel (Kim et al., 2005b).

2.4.3 Kallikrein-4 gene (*KLK4*)

KLK4 is mapped on 19q13.4 (Hart et al., 2004) and is expressed in ameloblasts and odontoblasts (Hu et al., 2000b; Nagano et al., 2003) during the transition and the maturation stages of amelogenesis (Hu et al., 2000b; Hu et al., 2002). KLK4 is a late protease which needs MMP-20 to remove a 6-amino-acid propeptide from the inactive zymogen form to the active form (Ryu et al., 2002). This calcium-independent serine protease plays a role in degrading the TRAP amelogenin cleavage to smaller products (Stephanopoulos et al., 2005). *KLK4* mutations lead to autosomal recessive hypomaturation AI (Hart et al., 2004), with clinical manifestation of normal

thickness enamel and yellow-brown discoloration. The mineral content in enamel is reduced, leading to decreased radiodensity (Hart et al., 2004) (Figure 2.8). Dental phenotypes of *MMP-20* and *KLK4* mutations share many similar clinical manifestations (Kim et al., 2005b).

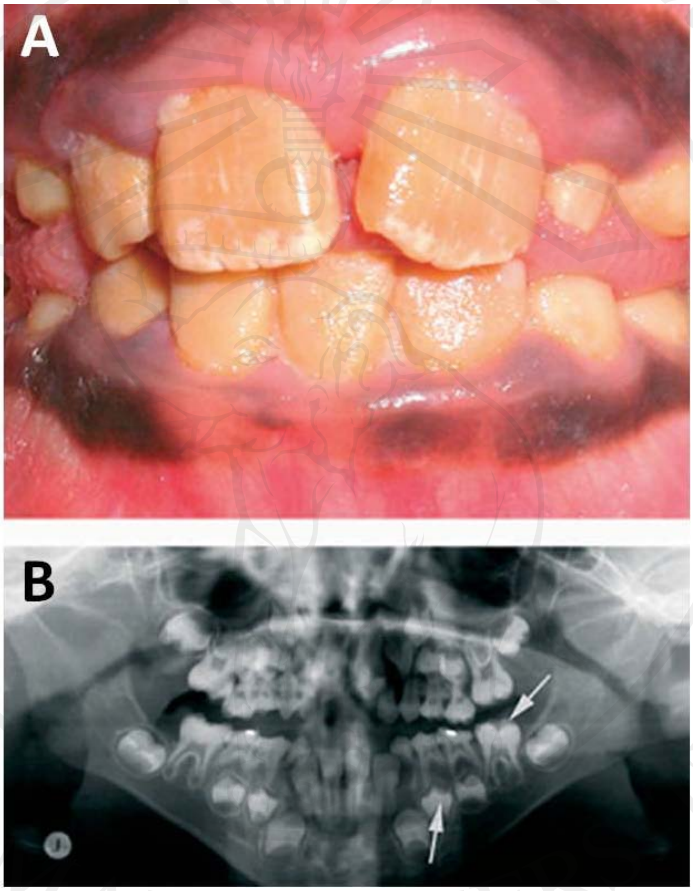

Figure 2.8 (A) Normal morphology of dental enamel with yellow-brown discoloration affecting both primary and permanent dentitions. (B) Radiographic examination shows enamel fracture of posterior teeth with reduction of enamel radiopacity. The opacity of enamel is a little greater than that of the underlying dentin (arrows), which is associated with the hypomineralisation of the enamel (Hart et al., 2004).

2.4.4 Family with sequence similarity 83 member H gene (*FAM83H*)

FAM83H is mapped on 8q24.3 (Lee et al., 2008). Expression of *Fam83h* in murine tooth development has been found in the ameloblasts of the developing tooth bud during the cap stage (Lee et al., 2009). Other studies have shown lower

expression of *Fam83h* in alveolar bone and odontoblastic cells (Lee et al., 2009). In ameloblasts, the expression level is high in the presecretory and secretory stages and low in the maturation stage of ameloblasts (Lee et al., 2009). This gene may play a role in the differentiation of ameloblasts from presecretory ameloblasts to functional ameloblasts, and also be involve in the calcification of the enamel matrix (Lee et al., 2009). Mutations of *FAM83H* present with autosomal dominant hypocalcified AI (Kim et al., 2008; Lee et al., 2008; Hart et al., 2009; Hyun et al., 2009). The thickness of the affected enamel of unerupted teeth is normal, but soon after eruption this soft, uncalcified enamel is worn by mastication (Kim et al., 2008; Lee et al., 2008; Hyun et al., 2009). Abraded teeth show yellow-brown, hypoplastic enamel with some residual enamel on the cervical part of the teeth (Hyun et al., 2009). The abraded surfaces of the teeth lead to tooth sensitivity to thermal changes (Lee et al., 2008; Hyun et al., 2009). Radiographic examination shows normal thickness of enamel, with reduced mineralization in developing teeth (Hyun et al., 2009) (Figures 2.9 and 2.10).

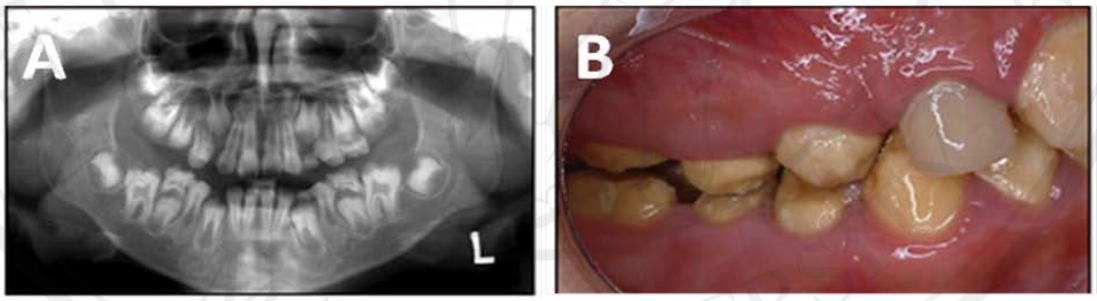

Figure 2.9 (A) Normal enamel thickness of unerupted teeth shown in the panoramic radiograph, (B) but the enamel is soft in consistency. The teeth are sensitive to thermal changes (Kim et al., 2008).

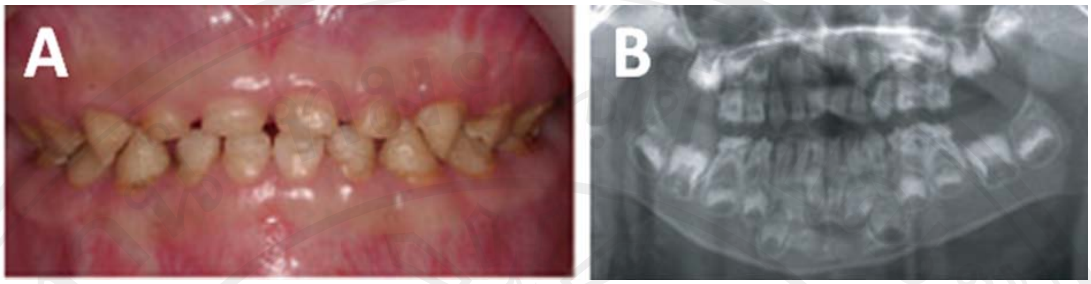

Figure 2.10 (A) Brown, hypoplastic, deciduous teeth with some islands of enamel on the cervical parts of mandibular anterior teeth. (B) Normal thickness with reduced mineralization in enamel of unerupted teeth is shown in the panoramic radiograph (Hyun et al., 2009).

2.4.5 Enamelin gene (*ENAM*)

2.4.5.1 *ENAM* and its structure

Human *ENAM* maps on 4q13.3 (Hu et al., 2000a). Murine *ENAM* consists of 10 exons and 9 introns (Hu et al., 2001b), whereas human *ENAM* consists of 9 exons and 8 introns (Hu et al., 2001b; Rajpar et al., 2001). Exon 2, present in mouse *ENAM*, is absent in human cDNA, but the intron separating the first and second exons in the human gene shows a sequence homologous to that of mouse exon 2, flanked by appropriate splice junctions (Hu et al., 2000b; Hu et al., 2001b; Hart et al., 2003a). The possibility of alternative splicing of the enamelin transcript is suggested (Hu et al., 2001b; Hart et al., 2003a).

ENAM is a tooth-specific gene with high expression in the enamel organ and low expression in odontoblasts (Hu et al., 2001b; Nagano et al., 2003; Wright, 2006). From one to five per cent of total enamel protein is enamelin (Fukae et al., 1996; Hu et al., 2001b), whose specific roles are still unclear. Immunohistochemistry has shown expression of enamelin during the secretory stage of amelogenesis throughout the entire thickness of dentino-enamel junction (DEJ) (Hu et al., 1997). Its expression disappears early in the maturation stage of amelogenesis (Hu et al., 1997).

A failure in crystallite elongation is presumably associated with a reduction of enamel thickness (Hu et al., 1997). When the intact (uncleaved) enamelin is restricted in its localization to the mineralization front, where it is important for crystal elongation, the enamel thickness is reduced (Hu et al., 1997). It is thought that

enamelin is important for enamel crystallite growth regulation and elongation in amelogenesis (Hu et al., 1997; Wright, 2006). Experiments in mice have shown expression of enamelin in the three stages of enamel formation and its expression halts before the expression of the amelogenin (Hu et al., 2001a).

2.4.5.2 Mutations in *ENAM*

ENAM is highly expressed in the ameloblasts during amelogenesis. It has been reported in several studies that *ENAM* mutations cause hypoplastic AI. Mutations were found in multiple locations (Figure 2.11 and Table 2.1).

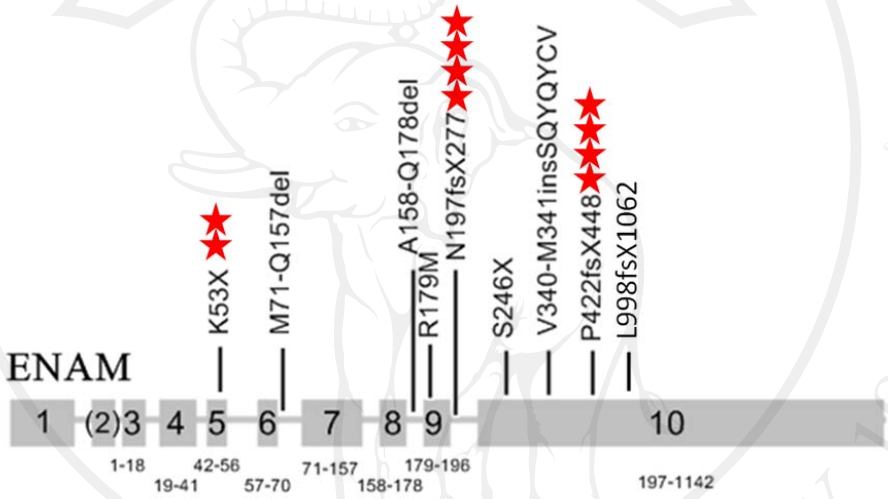

Figure 2.11 Schematic view of human *ENAM*. Black lines indicate amino acid changes and locations of known mutations. Number of stars indicates the frequency of reported mutations at each position.

Table 2.1 Previously reported mutations of human *ENAM* (Modified from (Pavlic et al., 2007).

Location	Genomic DNA	Proteins	Phenotype	Reference	Mode of inheritance
Exon 5	g.2382A>T	p.K53X	Local hypoplastic	Mårdh et al., 2002	AD
Exon 5	g.2382A>T	p.K53X	Local hypoplastic	Kim et al., 2006	AD
Intron 6	g.4806A>C	p.M71-Q157del	Generalized hypoplastic	Kim et al., 2005a	AD
Intron 8	g.6395G>A	p.A158-Q178del	Generalized hypoplastic	Rajpar et al., 2001	AD

Table 2.1 Previously reported mutations of human *ENAM* (Modified from (Pavlic et al., 2007). (continued)

Location	Genomic DNA	Proteins	Phenotype	Reference	Mode of inheritance
Exon9	g.8291G>T	p.R179M	Generalized hypoplastic	Gutierrez et al., 2007	AD
Intron 9	g.8344delG	p.N197fsX277	Generalized hypoplastic	Kida et al., 2002	AD
Intron 9	g.8344delG	p.N197fsX277	Generalized hypoplastic	Hart et al.,2003a	AD
Intron 9	g.8344delG	p.N197fsX277	Generalized hypoplastic	Kim et al., 2005a	AD
Intron 9	g.8344delG	p.N197fsX277	Generalized hypoplastic	Palvic et al., 2007	AD
Exon 10	g.12663C>A	p.S246X	Local hypoplastic	Ozdemir et al., 2005a	AD
Exon 10	g.12946-12947insAGTCAGTACCAGTACTGTGTC	p.V340-M341insSQYQYCV	Local hypoplastic	Ozdemir et al., 2005a	AD
Exon 10	g.13185-13186insAG	p.P422fsX448	Generalized hypoplastic	Hart et al., 2003b	AR/AD
Exon 10	g.13185-13186insAG	p.P422fsX448	Local hypoplastic	Ozdemir et al., 2005a	AD
Exon 10	g.13185-13186insAG	p.P422fsX448	Local hypoplastic	Palvic et al., 2007	AD
Exon 10	g.13185-13186insAG	p.P422fsX448	Generalized hypoplastic	Kang et al., 2009	AD
Exon 10	g.14971delT	p.L998fsX1062	Local hypoplastic	Kang et al., 2009	AD

g.6395G>A,IVS8+1G>A was the first reported heterozygous *ENAM* mutation which spoiled the intron 8 splice donor site (Rajpar et al., 2001). This mutation caused a severe form of autosomal dominant hypoplastic AI in both primary and permanent dentitions of affected members (Rajpar et al., 2001). The affected teeth showed very thin enamel thickness, and were small and yellow in color (Rajpar et al., 2001) (Figure 2.12).

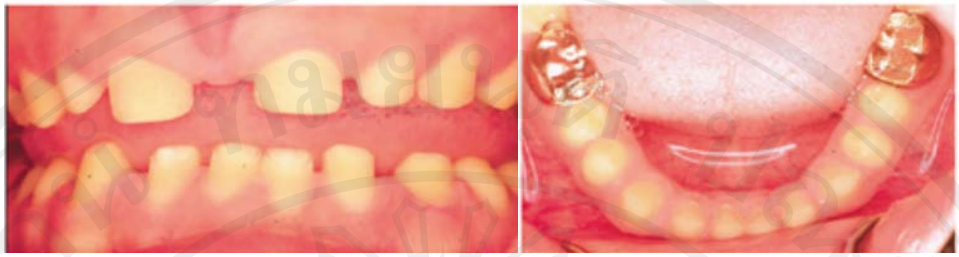

Figure 2.12 The affected teeth showed severe smooth hypoplastic enamel (Rajpar et al., 2001).

Mardh and colleagues reported an enamelin gene mutation in exon 5 (g.2382A>T, p.K53X) (Mardh et al., 2002). The clinical manifestation was reported as autosomal dominant local hypoplastic AI (Mardh et al., 2002). Affected enamel showed horizontal rows of pits and grooves or a large area of hypolplastic enamel (Mardh et al., 2002) (Figure 2.13).

Kida and colleagues reported a spontaneous mutation in *ENAM* (g.8344delG) in a Japanese family (Kida et al., 2002). The phenotype associated with this mutation was an autosomal dominant hypoplastic AI (Kida et al., 2002). The proband and his younger brother showed hypoplastic enamel on both dentitions with an anterior open bite (Kida et al., 2002). Their teeth were hypersensitive to cold stimuli (Kida et al., 2002). The affected father showed local hypoplastic enamel with horizontal lesions at the middle third of permanent teeth (Kida et al., 2002). His teeth had normal sensitivity to cold stimuli (Kida et al., 2002) (Figure 2.14).

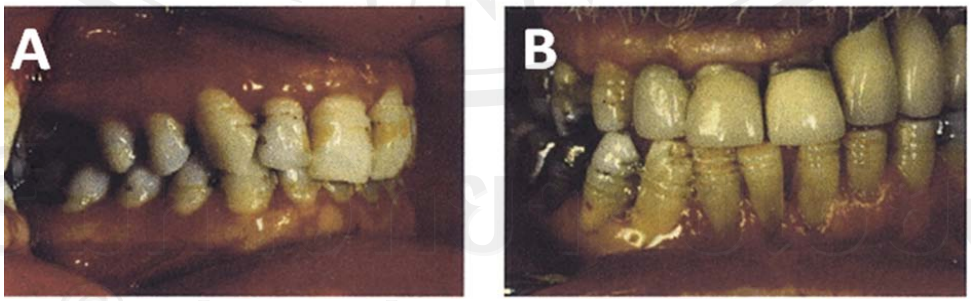

Figure 2.13 (A) Horizontal rows of pits and grooves or a large area of hypoplastic enamel in local hypoplastic AI. (B) Oral manifestation of an elderly relative of the left case showed similar enamel surfaces. The upper left teeth were crowned (Mardh et al., 2002).

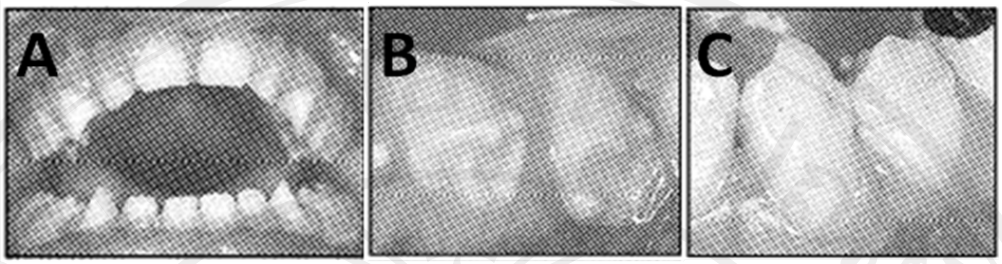

Figure 2.14 (A) Hypoplastic enamel with anterior open bite in primary teeth of a 3-year-old proband. (B) The lower right premolar teeth of the proband's brother were small and yellow in color. (C) The teeth of the father showed local hypoplastic enamel with horizontal lesions of enamel defect at middle third of the permanent teeth (Kida et al., 2002).

Hart and colleagues studied mutations of AI in 20 consanguineous families and found *ENAM* mutations in three families (g.13185_13186insAG) (Hart et al., 2003b). Three probands from different families homozygous for the g.13185_13186insAG showed severe generalized hypoplastic AI with radiographically undermineralized enamel, suggesting autosomal recessive AI in the probands (Hart et al., 2003b). Cephalometric analysis confirmed anterior open bite malocclusion, which was also found in these three affected probands (Hart et al., 2003b) (Figure 2.15). Localized enamel hypoplasia with variable patterns of enamel pitting, on the buccal surfaces of anterior teeth, or with enamel pits on cusps and occlusal surfaces of cuspids, premolars and molars, was found in both of each of the probands' parents, in one sibling of each proband, and also in many of their relatives (Hart et al., 2003b). The defective pits of hypoplastic enamel were approximately 1-2 millimeters in both depth and width (Hart et al., 2003b). The affected enamel was normal in color (Hart et al., 2003b). All individuals with localized enamel defects were heterozygous carriers of this mutation (Hart et al., 2003b). That report suggested that the g.13185_13186insAG mutation in *ENAM* resulting in localized hypoplastic enamel pitting is a dominant trait and that the anterior open bite malocclusion with hypoplastic AI is a recessive trait (Hart et al., 2003b) (Figure 2.16).

The g.8344delG mutation in exon 9 of *ENAM* was also found in a Lebanese family by Hart and colleagues (Hart et al., 2003a). This report found autosomal-dominant generalized hypoplastic AI (Hart et al., 2003a). The affected enamel

showed variable phenotypes in affected individuals, ranging from rough to smooth surface enamel with horizontal rows of shallow pits (Hart et al., 2003a) (Figure 2.17).

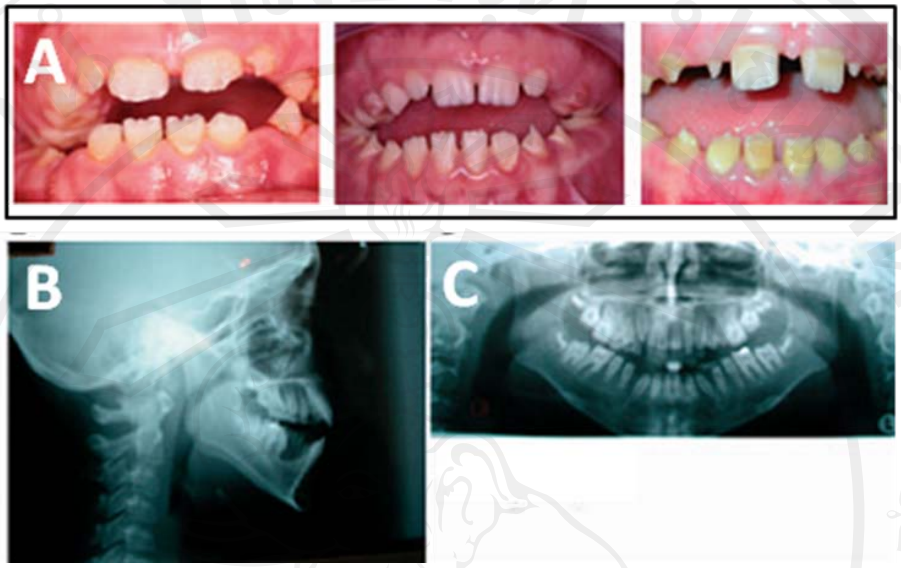

Figure 2.15 (A) Three probands from different families shows generalized hypoplastic enamel with clinically anterior openbite malocclusion. (B) The cephalometric radiograph in one of the proband shows anterior open bite. (C) The panoramic radiograph shows generalized hypoplastic enamel with reduction in radiodensity of enamel (Hart et al., 2003b).

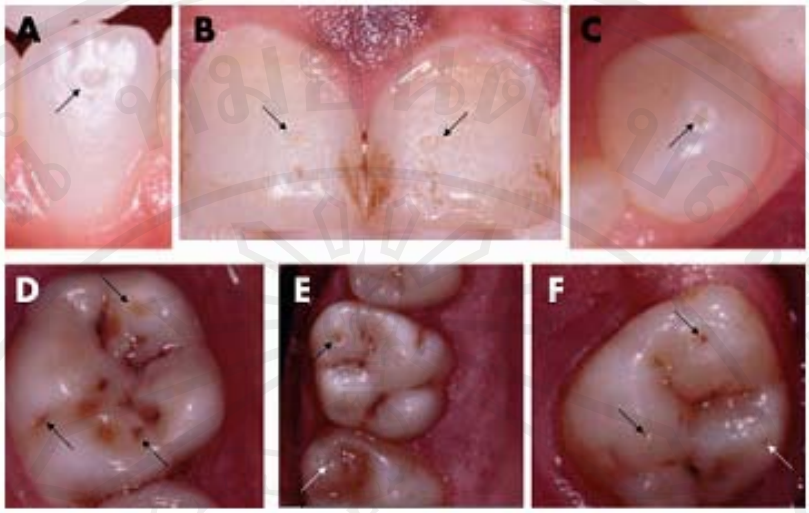

Figure 2.16 Heterozygous carriers (probands'parents, three siblings and also three of their relatives) of g.13185_13186insAG in an *ENAM* mutation showed localized enamel pitting on (A and B) buccal surfaces of anterior teeth, (C) enamel pit on cusp and occlusal surface canines, (D to F) premolars and molars (Hart et al., 2003b).

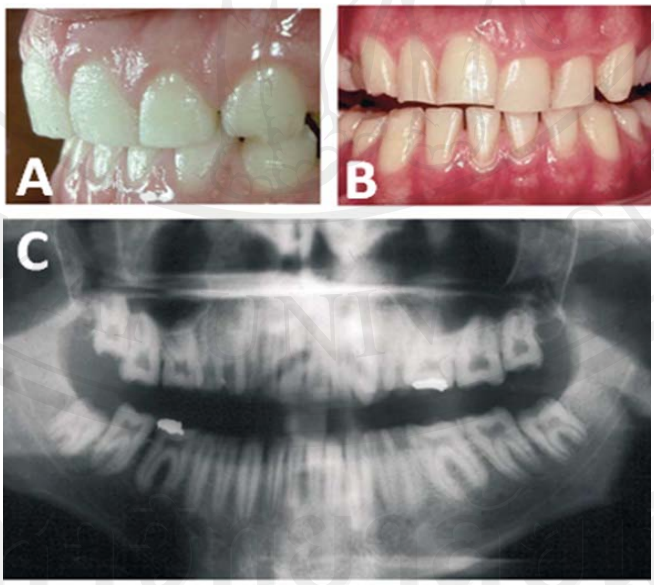

Figure 2.17 (A and B) Both affected individuals showed generalized hypoplastic enamel. (A) The dentition of the proband showed shallow horizontal pits on enamel while (B) the dentition of the relative showed smooth, worn enamel. (C) The radiographic examination of the relative showed very thin to absent enamel (Hart et al., 2003a).

Two *ENAM* mutations, one novel (g.4806A>C, IVS6-2A>C) and one previously reported (g.8344delG), in two families with hypoplastic autosomal dominant AI were reported by Kim and colleagues (Kim et al., 2005a). This study reported a previously identified mutation (g.8344delG), which was found in an Iranian family (Kim et al., 2005a). The 11-year-old male proband showed anterior open bite with jagged incisal edges (Kim et al., 2005a). Affected enamel was thin and yellow, with shallow horizontal grooves on the buccal surfaces of the anterior teeth, whereas normal enamel was found on the cusp tips and marginal ridges of the posterior teeth and at the incisal line angles of the anterior teeth (Kim et al., 2005a). Because the mutation in *ENAM* (g.8344delG) was previously reported (Kida et al., 2002; Hart et al., 2003a), this report suggested a generalized hypoplastic enamel with variations in surface texture ranging from smooth surface with or without shallow grooves, to horizontal rows of shallow pits on rough enamel as the common finding in this same mutation from three families (Kim et al., 2005a) (Figure 2.18).

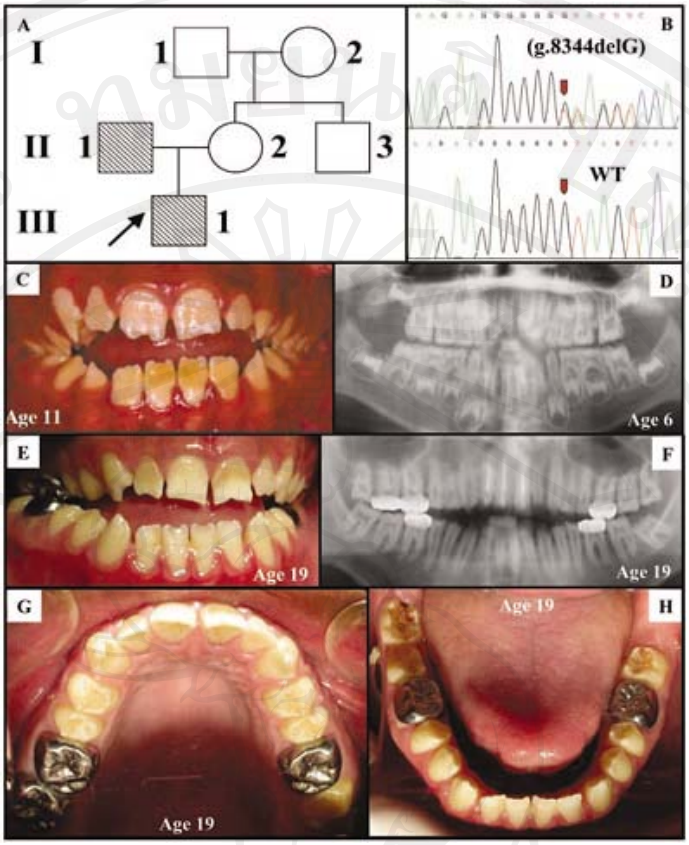

Figure 2.18 (A) Pedigree of the family. (B) DNA sequencing chromatograms of the mutation (g.8344delG) and the corresponding wild-type (WT) sequence. (C and D) Clinical manifestation and the radiographic examination of the proband at 11 and 6 years of age, respectively. (E to H) Intraoral photographs and the panoramic radiograph of the proband at 19 years of age. The upper anterior teeth were endodontically treated teeth with composite restorations (Kim et al., 2005a).

Kim and colleagues also reported another novel mutation in the splice acceptor site at the end of intron 6 of *ENAM* (g.4806A>C,IVS6-2A>C) in another family (Kim et al., 2005a). A 12-year-old female proband showed generalized, rough and thin enamel with horizontal grooves of hypoplastic enamel on yellowish-hued crowns (Kim et al., 2005a). Her teeth were sensitive to thermal changes (Kim et al., 2005a). The same mutation was also identified in the proband's mother and brother (Kim et al., 2005a) (Figure 2.19).

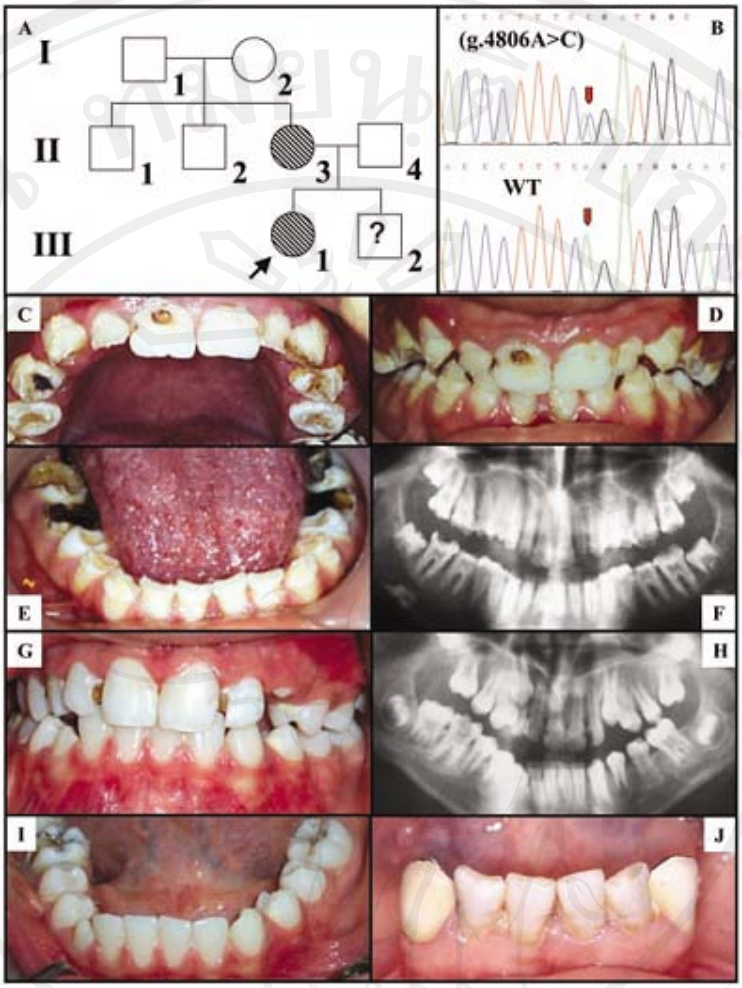

Figure 2.19 (A) Pedigree of the family. (B) DNA sequencing chromatograms of the novel mutation (g.4806A>C) and the corresponding wild-type (WT) sequence. (C to F) Clinical manifestation and the radiographic examination of the proband at age 12.5. (G to I) Intraoral photographs and the panoramic radiograph of the proband's younger brother at age 11. (J) Mandibular anterior teeth of the proband's mother (Kim et al., 2005a).

Ozdemir and colleagues sequenced *ENAM* in 10 Turkish families with autosomal hypoplastic AI and two mutations were found in two families (Ozdemir et al., 2005a). A novel nonsense mutation (g.12663C>A; p.S246X) was identified in one family, in which the 16-year-old proband showed autosomal dominant local hypoplastic AI (Ozdemir et al., 2005a). The proband showed localized enamel hypoplasia with composite laminate restorations on maxillary and mandibular anterior teeth without anterior open bite (Ozdemir et al., 2005a). The proband's father, grandfather, aunt

and cousin showed hypoplastic AI, while the proband's mother and two other siblings were unaffected, which suggested autosomal dominant transmission (Ozdemir et al., 2005a) (Figure 2.20). Another mutation was reported in another family, in which both parents were carriers of AI (Ozdemir et al., 2005a). A novel 21-base-pair insertion mutation in *ENAM* (g.12946_12947insAGTCAGTACCAGTACTGTGTC/ WT; p.V340_M341insSQYQYCV) was identified in the father and a two-base-pair insertion mutation (g.13185_13186insAG; p.P422fsX448) was identified in the mother (Ozdemir et al., 2005a). The 10-year-old female proband, who had compound heterozygotes of these two enamelin gene mutations, presented with generalized hypoplastic AI with anterior open bite. The eldest sibling showed a similar phenotype of generalized hypoplastic AI, but without anterior open bite (Ozdemir et al., 2005a). Localized and circumscribed enamel pitting was found in the proband's parents and in other siblings (Ozdemir et al., 2005a). That report suggested that a novel insertion mutation in the enamelin gene (g.12946_12947insAGTCAGTACCAGTACTGTGTC /WT) is dose-dependent, with mild, localized enamel pitting as a dominant trait, and generalized hypoplastic AI, which is a more severe phenotype, as a recessive trait (Ozdemir et al., 2005a) (Figure 2.21).

Gutierrrez and colleagues reported an *ENAM* mutation in exon 9 (g.817G>T) of nine members of one family. The mutation led to a substitution of arginine with methionine in codon 179 (R179M) (Gutierrez et al., 2007). The affected members showed autosomal dominant hypoplastic AI with grooves and irregularities on thin enamel of honey-yellowish colored teeth (Gutierrez et al., 2007). There were horizontal slits in lower anterior teeth with some fewer vertical slits in upper anterior teeth (Gutierrez et al., 2007). All affected members had tooth sensitivity to thermal changes (Gutierrez et al., 2007). The radiographic examination showed some differences, such as dilacerations in normal-sized roots and dwarf roots in some members (Gutierrez et al., 2007) (Figure 2.22).

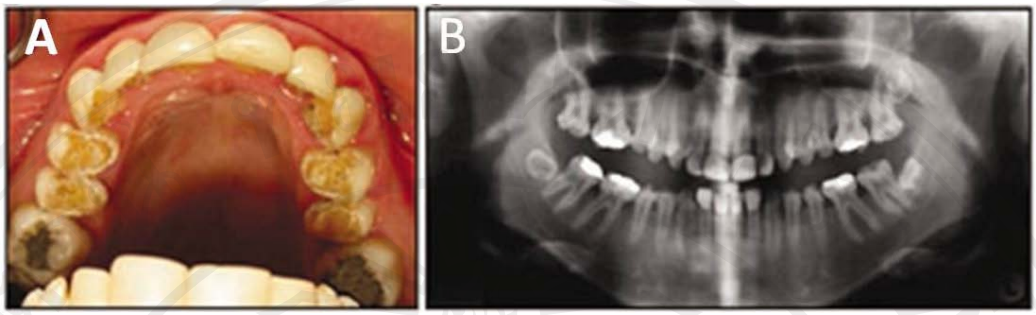

Figure 2.20 (A) Intraoral photograph of the proband shows hypoplastic enamel with composite laminate restorations on maxillary anterior teeth. (B) The panoramic radiograph shows local hypoplastic enamel with reduction in radiodensity of enamel compared with dentin (Ozdemir et al., 2005a)

Recently, Kang and colleagues reported the latest *ENAM* mutation of hypoplastic enamel in two Turkish families (Kang et al., 2009). The first family showed a local hypoplastic phenotype (Kang et al., 2009). The affected mother showed typical horizontal grooves of hypoplastic enamel at the middle to the cervical third of the crowns (Kang et al., 2009). The daughter showed small hypoplastic spots on wide, irregular bands of hypoplastic enamel (Kang et al., 2009). The frameshift mutation in exon 10 (g.14917delT, p.L998fsX1062), which resulted in 64 novel amino acids, was identified in this family (Kang et al., 2009). That report suggested that lack of a C-terminus in the mutation, which may play a role in crystallite formation, may relate to the thinness of the enamel (Kang et al., 2009). Another possibility is that the novel 64 amino acids may resist and interfere with enamel formation and growth of the crystal through a dominant-negative effect (Kang et al., 2009) (Figure 2.23).

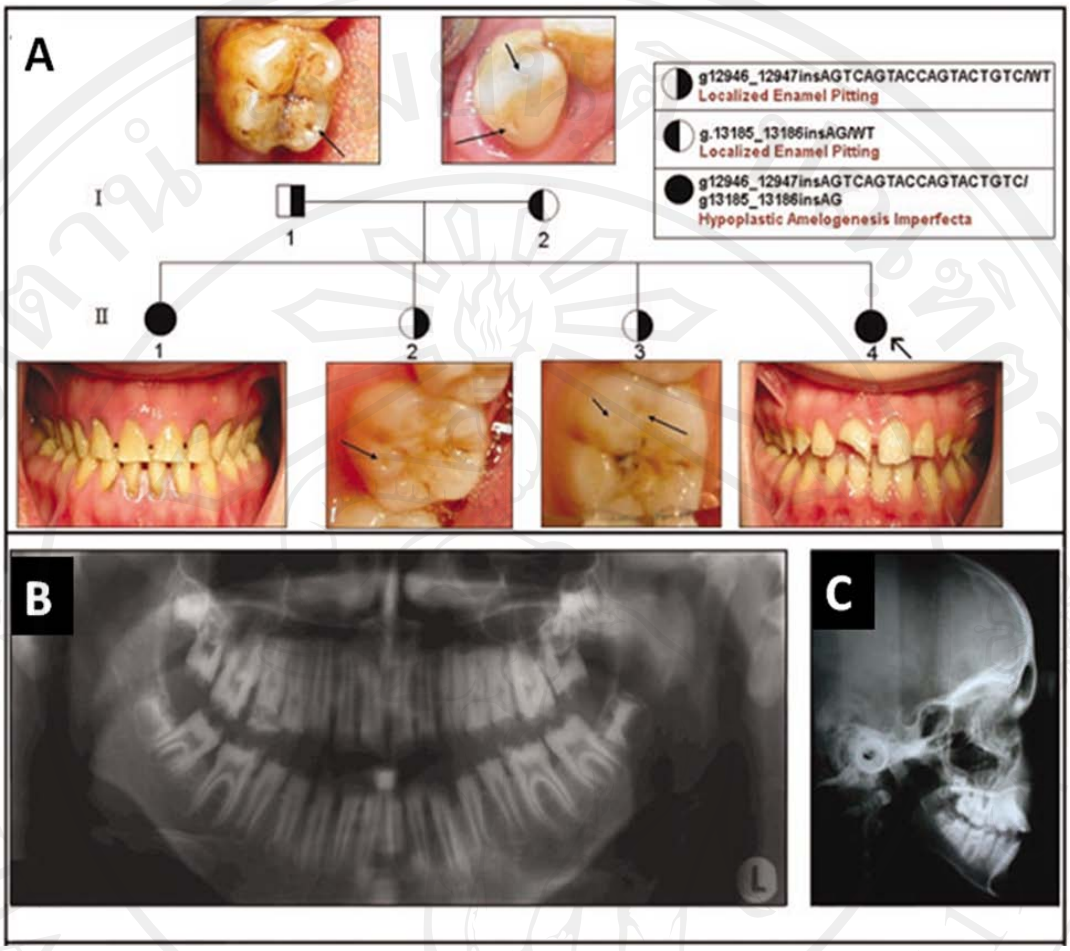

Figure 2.21 (A) Pedigree of the family with *ENAM* mutations (g.12946_12947insAGTCAGTACCAGTACTGTGTC/WT;p.V340_M341insSQYQYCV and g.13185_13186insAG; p.P422fsX448). Clinically localized enamel pitting was found in the individuals with either left- or right-shaded symbols (I-1, I-2, II-2, II-3) while the generalized hypoplastic AI was found in the completely shaded individuals who were compound heterozygotes (II-1, II-4). (B) Generalized hypoplastic AI in the panoramic radiograph of the proband (II-4). (C) Anterior open bite in the proband, (II-4) which was confirmed by lateral cephalometric radiograph (Ozdemir et al., 2005a).

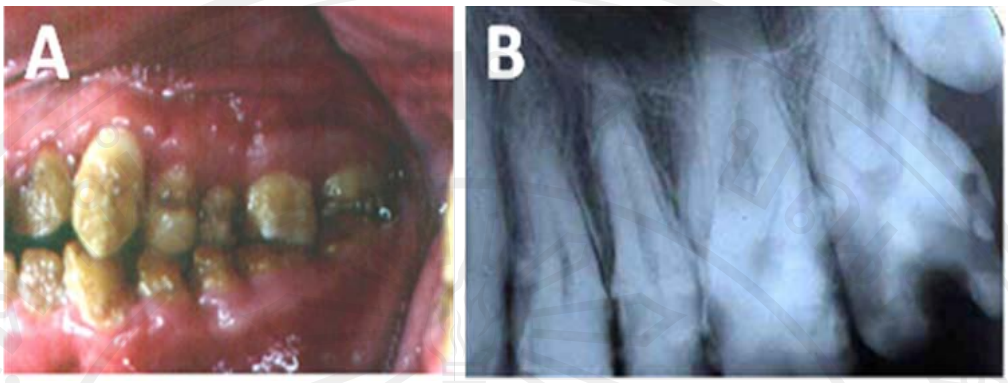

Figure 2.22 (A) The clinical manifestation showed generalized hypoplastic enamel with some horizontal and vertical grooves on enamel. (B) The radiographic examination shows dilaceration in normal-sized root tooth (Gutierrez et al., 2007).

The second Turkish family which was reported by Kang and colleagues showed generalized hypoplastic enamel and anterior open bite in the proband, who had a homozygous mutation in exon 10 (g.13185_13186insAG, p.P422fsX448) which has been reported previously (Hart et al., 2003b; Pavlic et al., 2007; Kang et al., 2009). The proband also showed taurodontism in several of her second molars, whereas no enamel phenotype of AI was found in either of her parents or other siblings, all of whom were heterozygous carriers (Kang et al., 2009). No disease-causing mutations were found in *DLX3* (Kang et al., 2009) (Figure 2.24).

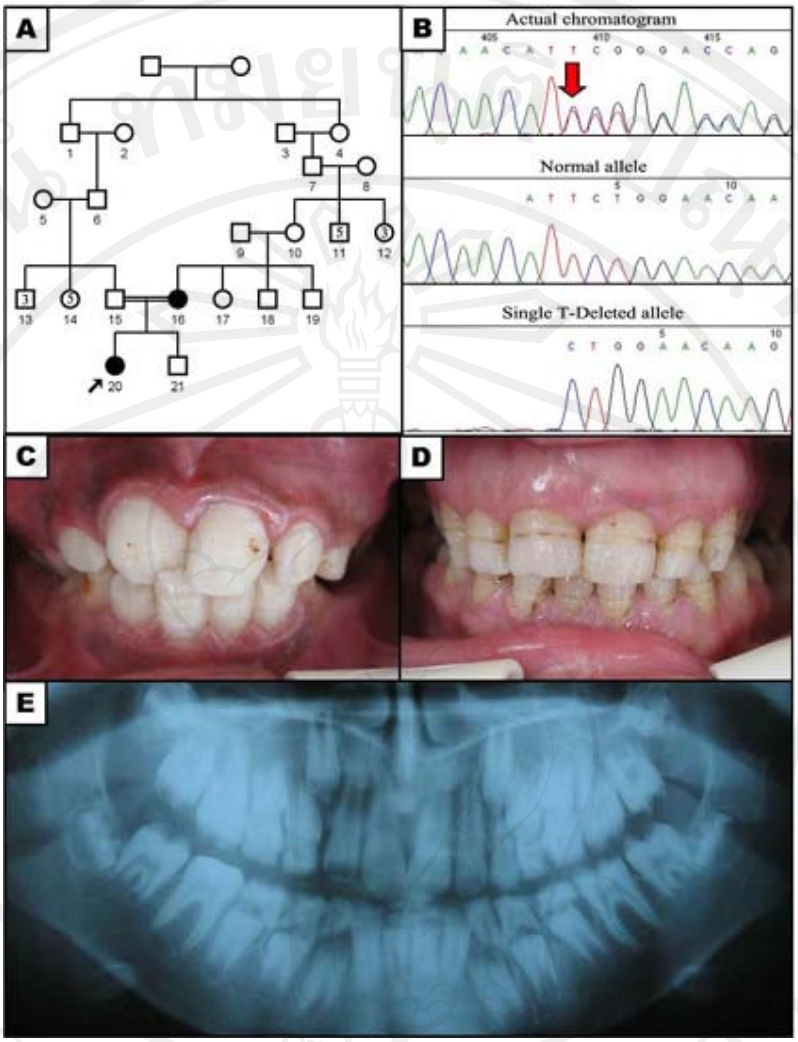

Figure 2.23 (A) Pedigree of family 1 with *ENAM* mutation (g.14917delT, p.L998fsX1062). (B) Sequencing chromatogram of the affected proband; the red arrow shows the position of T deletion. The lower panel shows a mutated allele. (C) Frontal view of proband's affected teeth shows small hypoplastic spots on wide irregular, hypoplastic bands of enamel. (D) Frontal view of affected mother shows typical horizontal grooves of hypoplastic enamel at the middle to the cervical third of the crowns. (E) Panoramic radiograph of the proband's teeth (Kang et al., 2009).

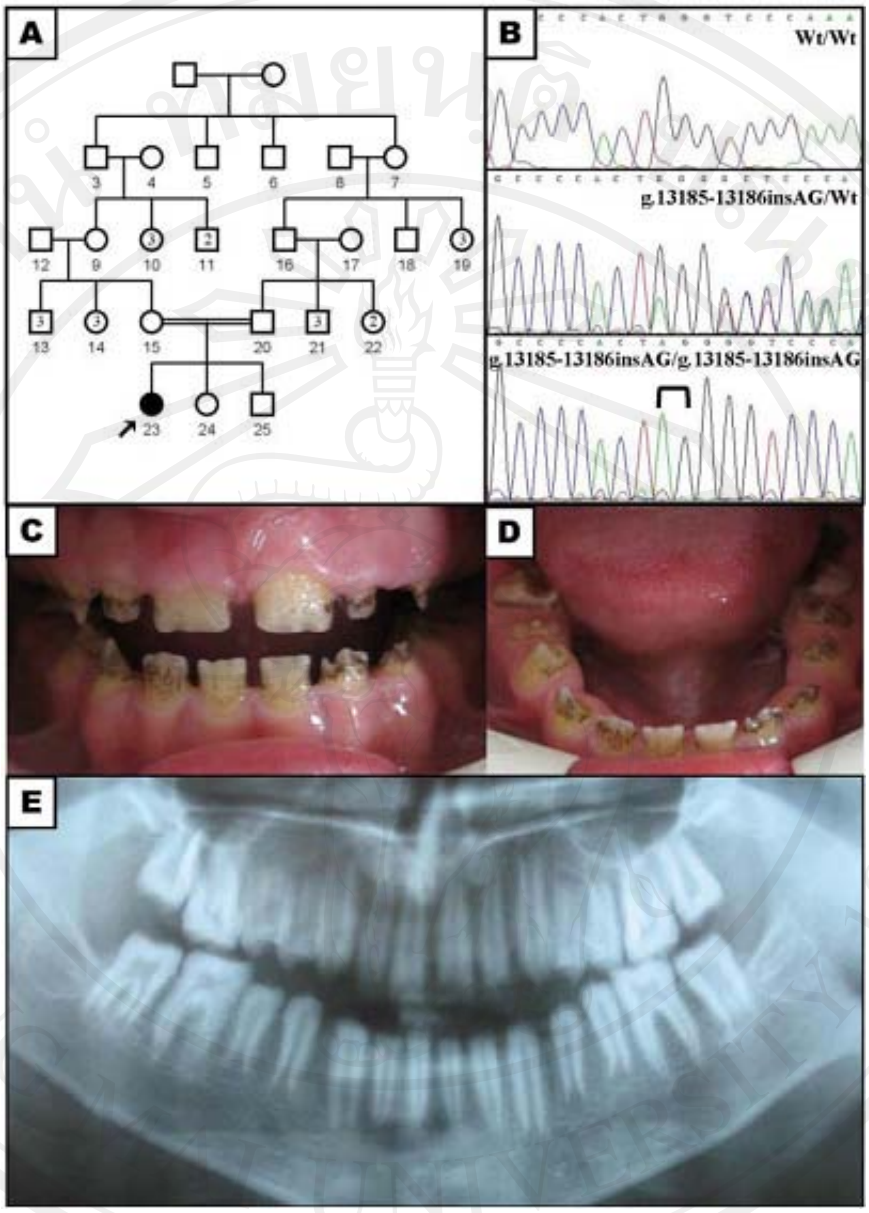

Figure 2.24 (A) Pedigree of family 2 with *ENAM* mutation (g.13185_13186insAG, p.P422fsX448). (B) Sequencing chromatogram of the normal control is in the upper panel, while the chromatogram of the heterozygous g.13185_13186insAG mutation is in the middle panel. The homozygous g.13185_13186insAG mutation (proband) is in the lower panel. (C to E) Oral manifestation of generalized hypoplastic enamel in the proband and panoramic radiograph of the proband's teeth (Kang et al., 2009).